

# Failure Criterion of Lightweight Aggregate Concrete Subjected to Triaxial Compression

By

Yoshiji NIWA\*, Shoichi KOBAYASHI\* and Wataru KOYANAGI\*

(Received December 28, 1966)

Based on the theoretical studies on the failure of homogeneous isotropic brittle materials, failure criteria of the materials under combined stresses are represented as convex surfaces in the principal stress space.

The failure surface of lightweight aggregate concrete was determined experimentally through uniaxial, biaxial and triaxial compression tests with about two hundred of 10.5 cm cube specimens.

The surface is convex and has the space diagonal as a threefold rotation axis. The surface expands with an increase of hydrostatic pressure. The right sections of the surface are slightly bulged from equilateral triangles and become more bulged as hydrostatic pressure increases.

## 1. Introduction

Knowledge of failure criteria of concrete subjected to combined stresses is of basic importance for evaluating the safety factors of structures. A lot of work has been devoted to obtain the failure criteria, though so far a general triaxial test has never been done.

In the present paper authors are chiefly concerned with a multiaxial compression test.

A possible failure criterion of brittle materials will be discussed at first, then the experimental failure criterion for lightweight aggregate concrete will be established.

## 2. Fundamental Properties of Failure Criteria

Generalized stresses (forces, stresses and stress rates etc.) and generalized strains (displacements, strains and strain rates etc.) of materials or of a system of materials can be expressed as a point in the generalized stress and strain space. If the stresses and the strains at failure or collapse are obtainable, the failure or collapse can be completely expressed by a single point in the stress and strain space.

---

\* Department of Civil Engineering.

A set of such points forms a failure surface, which must be determined by experiment for each material, or for each system of materials.

In what follows, our discussion will be limited to brittle materials or a system of brittle materials. As the generalized stress-strain relations of brittle materials may be uniquely obtained, the failure surface of such materials will be a function of the stresses only. If the materials are strain-rate insensitive, the surface must be convex in the stress space owing to the Drucker's postulate of stability of materials as mentioned elsewhere<sup>1)~3)</sup>. The convexity of the failure surface of brittle materials or of the system of brittle materials is the most fundamental. It is valid for any materials whether they are continuous or discontinuous, or linear or non-linear, provided that they are stable. For a special case that brittle materials or the system of brittle materials are assumed to be independent of the previous history, the failure surface must be fixed in the stress space. In addition to this assumption, if the isotropy and homogeneity of the materials in macroscale are assumed, the failure surface can be expressed in the principal stress space  $(\sigma_1, \sigma_2, \sigma_3)$  as a convex surface with space diagonal  $(\sigma_1 = \sigma_2 = \sigma_3)$  of its three-fold rotation axis. Based on the extended Griffith and the modified Griffith theories into three dimensions, the following failure surface is concluded<sup>1)~3)</sup>.

The failure surface is composed of a set of three planes expressed as  $\min(\sigma_1, \sigma_2, \sigma_3) = -K$  (compressive stress is taken positive and  $K$  is the uniaxial tensile strength) and of six curved surfaces which are connected with one another on the planes of  $\sigma_1 = \sigma_2$ ,  $\sigma_2 = \sigma_3$  and  $\sigma_3 = \sigma_1$  and expand with an increase of hydrostatic pressure. The former and the latter are smoothly connected with each other. The right sections (sections of the failure surface cut out by planes of  $I_1 = \sigma_1 + \sigma_2 + \sigma_3 = \text{const.}$ ) of the former are equilateral triangles and those of latters are slightly bulged from equilateral triangles. The Rendulic stress curves (a section of the failure surface cut out by a plane containing the space diagonal and one of the principal stress axis) are straight lines of constant tensile strength for the region of maximum stress less than  $3K$  and straight or slightly curved lines for the region of the minimum stress greater than  $(-K)$ .

The sketch of the failure surface is shown in Fig. 1. The right sections and Rendulic stress curves are shown in Fig. 2 and Fig. 3, respectively. Owing to the isotropy one-sixth of the surface, i.e. the region  $|\theta| \leq 30^\circ$  in Fig. 2, is sufficient to determine the entire surface. If the stresses at failure  $(\sigma_1 \geq \sigma_2 \geq \sigma_3)$  are obtained, the length  $r$  and  $\theta$  on the right sections in Fig. 2 are determined by

$$r = \sqrt{\frac{1}{3} \{(\sigma_1 - \sigma_2)^2 + (\sigma_2 - \sigma_3)^2 + (\sigma_3 - \sigma_1)^2\}} = \sqrt{3} \tau_{oct} = \sqrt{\frac{2}{3} (I_1^2 - 3I_2)} \quad (1)$$

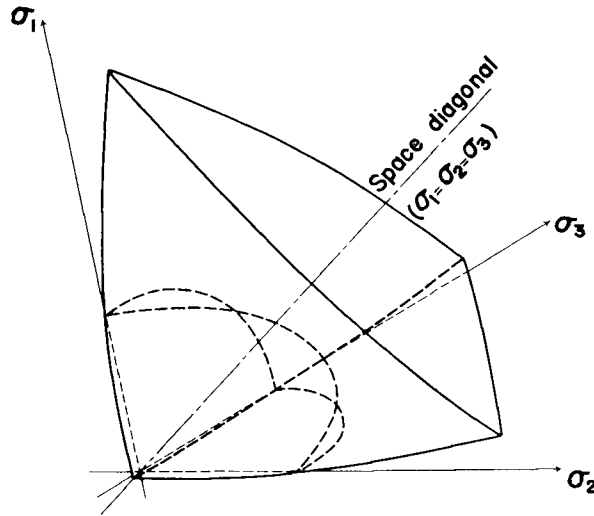


Fig. 1. Sketch of failure surface.

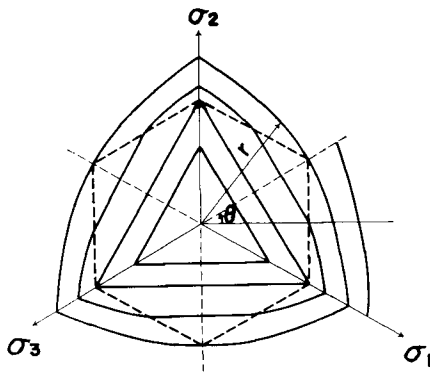


Fig. 2. Sketch of right sections.

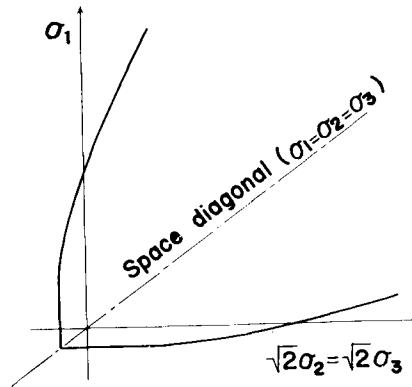


Fig. 3. Sketch of Rendulic stress curves.

and

$$\theta = \tan^{-1} \left( \frac{1}{\sqrt{3}} \cdot \frac{2\sigma_2 - \sigma_1 - \sigma_3}{\sigma_1 - \sigma_3} \right), \quad (2)$$

where  $I_1 = \sigma_1 + \sigma_2 + \sigma_3$ ,  $I_2 = \sigma_1\sigma_2 + \sigma_2\sigma_3 + \sigma_3\sigma_1$ .

In the determination of right sections the selected several experiments for  $I_1 = \text{const.}$  may be sufficient, since the convexity of the surface is guaranteed.

### 3. Experimental Work

#### 3.1. Test specimens

The lightweight aggregate concrete reported herein was made of ordinary

portland cement (JIS R 5210-64) and pelletized lightweight gravel and sand. The coarse aggregate was Lionite gravel, 15 mm maximum size and specific gravity 1.53. The fine aggregate was Lionite sand, average fineness modulus 2.99 and specific gravity 1.98. The mix was 1.00:1.34:1.43 with water-cement ratio of 44.5 percent and the slump measured was 4~6 cm.

Sixteen 10.5 cm cube specimens and six  $\phi 10 \times 20$  cm cylinder specimens were casted in steel molds from the same batch. The cube specimens were finished with polished glass plates about three hours after casting and the cylinder specimens were capped with neat cement paste after one day. After the removal of the molds, all the specimens were cured in water and one day in air in the moisture room (temperature  $20^{\circ} \pm 1^{\circ}\text{C}$ , relative humidity  $90 \pm 5\%$ ). Specimens were thus tested at 28 days.

### 3.2. Test procedure

Cube specimens were tested by use of Riehlé type triaxial compression test equipment, whose capacities are 200 tons in vertical and 100 tons in two orthogonally located horizontal directions (Fig. 4)<sup>1)</sup>.

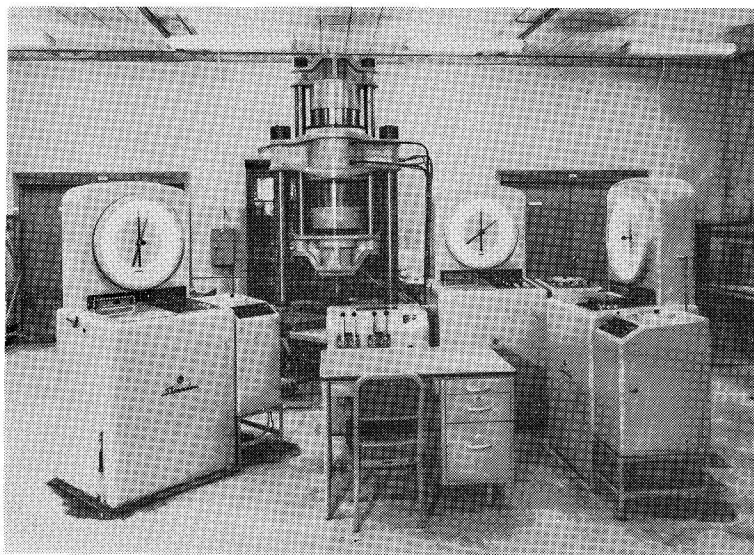
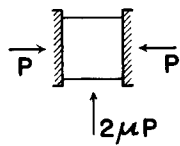


Fig. 4. Triaxial test equipment.

It is widely known that the friction between platen and end surface of specimens has a great influence on the compressive strength. Special care has been taken to reduce the friction. Coefficients of the friction of several lubricants examined in the preliminary test with the same cube specimens in the range of stresses about 20

Table 1. Apparent Coefficient of Friction.

Lubricants	Apparent Coefficient of Friction	Remarks
None	0.46 ~0.65	
Graphite powder	0.28 ~0.31	
Cup grease	0.15 ~0.24	
Tefron sheet (0.05 mm thick) + silicon grease	0.018~0.023	
Rubber sheet (0.23 mm thick) + silicon grease	0.008~0.012	

to 95 percent of uniaxial compressive strength are listed in Table 1. The soft thin rubber sheet (0.23 mm thick) applied with silicon grease is very effective. The coefficient with it is about 2 percent of that without any lubricant. The appropriateness of using the rubber sheet with silicon grease was confirmed, as will be discussed later, by the uniaxial compressive strength and the failure pattern of cube specimens. Throughout the tests the rubber sheet applied with silicon grease is used.

The partial loading on the 10.5 cm cube specimens by  $10 \times 10$  cm square platen was found to have no significant effect even on uniaxial compressive strength, provided that the faces of the specimens were well lubricated. Thus, all the results were regarded as those under uniform pressure.

Cylinder specimens were tested in order to obtain the crushing strength and split strength and also to find variations between batches.

The tests were carried out on the following program.

(i) Uniaxial compression test;

Uniaxial tests of cube specimens were carried out in order to compare the strength of the cube specimens with that of the cylinder specimens. Loading rate was  $3 \sim 4$  kg/cm<sup>2</sup>/sec. Extreme care was exerted to eliminate eccentricity.

(ii) Biaxial compression test;

Specimens were mainly tested by proportional loading, i.e. the ratios of the principal stresses were kept constant ( $\sigma_1/\sigma_2 = 1/9, 1/4, 1/2, 3/4$  and 1) while loading. Several loading paths shown in Fig. 5 were also traced in order to examine the effect of loading history on the strength. Loading rate was  $3 \sim 4$  kg/cm<sup>2</sup>/sec. for the maximum stress.

(iii) Triaxial compression test;

In order to obtain the right sections of the failure surface accurately, most tests were carried out in such a way that the sum of the principal stresses ( $I_1$ ) was kept constant. Loading paths are shown in Fig. 6, i.e. the loads were increased

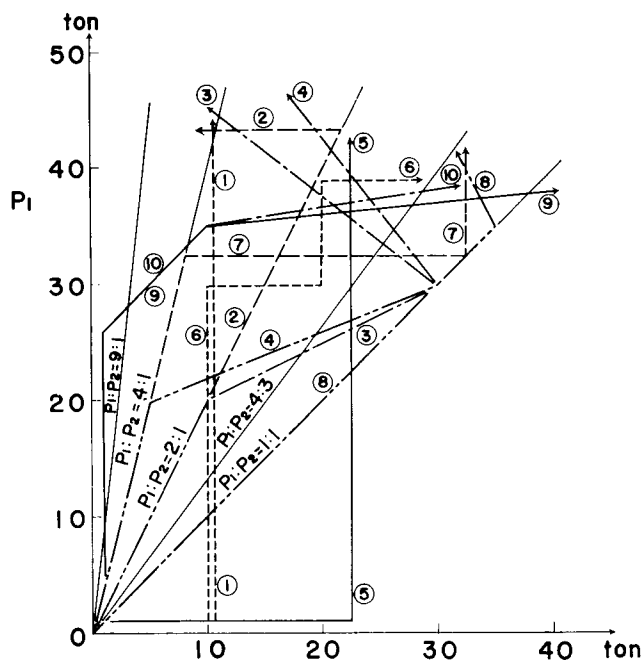


Fig. 5. Loading paths (Biaxial test).

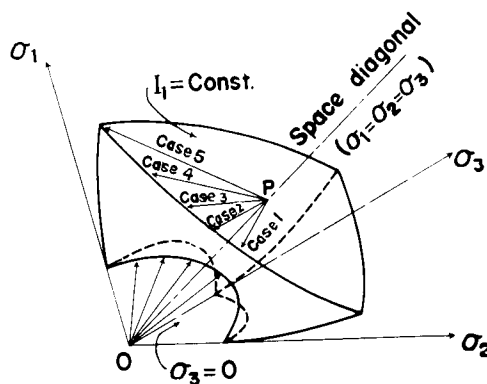


Fig. 6. Loading paths.

along the space diagonal  $\overline{OP}$  and then varied with proportional load increment in the plane of  $I_1 = \text{const.}$  Five paths from Case 1 ( $\sigma_1 = \sigma_2 \geq \sigma_3$ ) to Case 5 ( $\sigma_1 \geq \sigma_2 = \sigma_3$ ) were examined. The sums of the applied loads were chosen 54, 72, 108, 144, 180 and 216 tons, which are denoted by Series A, B, C, D, E and F, respectively. These sums of the principal stresses are about 1.5, 2.1, 3.2, 4.3, 5.4 and 6.5 times the uniaxial compressive strength, respectively, as will be

shown later. The proportional loading and the sequent loading, in which the successively smaller loads were kept constant and the rest of the loads was increased to failure, were also examined. Loading rates were about  $4\sim 6 \text{ kg/cm}^2/\text{sec}$ . along the space diagonal and about  $3 \text{ kg/cm}^2/\text{sec}$ . for the maximum stress along other paths.

## 4. Results and Discussions

### 4.1. Uniaxial compression test

Uniaxial crushing strength and split strength of cylinder specimens were  $316 \text{ kg/cm}^2$  (mean value of 27 specimens) with the coefficient of variation 6.3 percent and  $29.7 \text{ kg/cm}^2$  (mean value of 25 specimens) with the coefficient of variation 8.1 percent, respectively. Uniaxial compressive strength ( $\sigma_0$ ) of cube specimens was  $298 \text{ kg/cm}^2$  (mean value of 16 specimens) with the coefficient of variation 7.0 percent.

In uniaxial compression test specimens burst into pieces of column parallel to the direction of load as shown in Fig. 7a. In comparison with this, the failure pattern obtained by the ordinary compression test is shown in Fig. 7b. In the

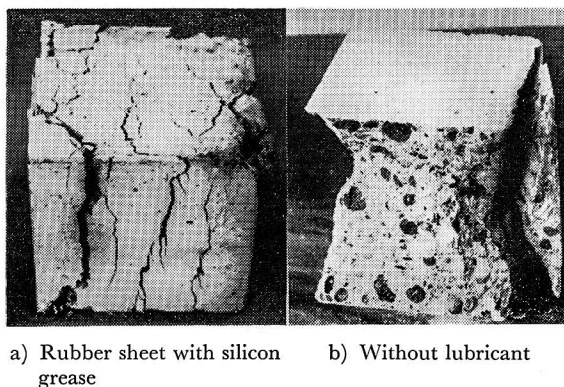


Fig. 7. Failure patterns (Uniaxial).

former test the friction between the platen and the end of specimens is reduced extremely ( $\mu \doteq 0.01$ ), whereas it is not in the latter. The crushing strength of the latter is much higher than that of the cylinder specimen, while the compressive strength of the former is almost equal to the cylinder strength. Judging from this fact and the failure pattern, the compressive strength obtained herein can be regarded as an uniaxial compressive strength.

### 4.2. Biaxial compression test

Test results are plotted in Fig. 8. In the same figure the results obtained by

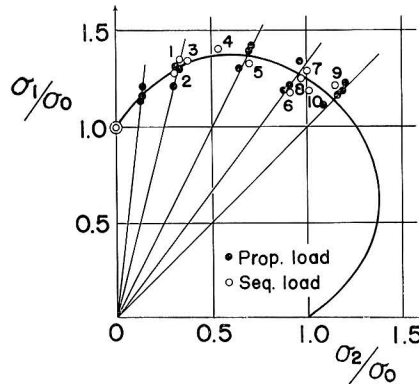


Fig. 8. Test results (Biaxial).

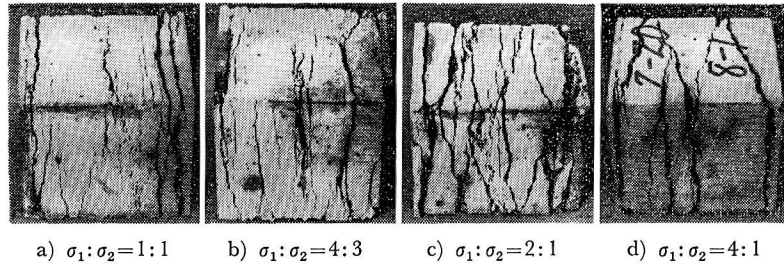


Fig. 9. Failure patterns (Biaxial).

the loading paths in Fig. 5 are also plotted with path numbers. All the specimens burst into thin layers parallel to the direction of loads as shown in Fig. 9.

The maximum principal stress ( $\sigma_1$ ) varies with an increase of intermediate stress ( $\sigma_2$ ). At  $\sigma_2/\sigma_0=0.7$ , the maximum stress  $\sigma_1/\sigma_0=1.4$  is attained and at  $\sigma_1=\sigma_2$ ,  $\sigma_1/\sigma_0=\sigma_2/\sigma_0=1.2$ . Fig. 8 also shows that the loading path has no significant effect on the biaxial compressive strength.

The curve obtained here by biaxial compression tests is the intersection of the failure surface and a plane of  $\sigma_3=0$ .

#### 4.3. Triaxial compression test

The failure was defined here in such a way that the loads had changed suddenly.

Right sections and Rendulic stress curves are shown in Figs. 10 and 11, respectively. Relations between  $\sqrt{3} \tau_{oct}/\sigma_0 = \sqrt{\frac{2}{3} (I_1^2 - 3I_2)} / \sigma_0$  and  $I_1/\sigma_0$ ,  $(\sigma_1 + \sigma_3)/\sigma_0$  and  $(\sigma_1 - \sigma_3)/\sigma_0$ , and  $I_1/\sigma_0$  and  $(\sigma_1 + \sigma_3)/\sigma_0$ , are shown in Figs. 12, 13 and 14, respectively. Typical failure patterns are shown in Figs. 15 and 16.



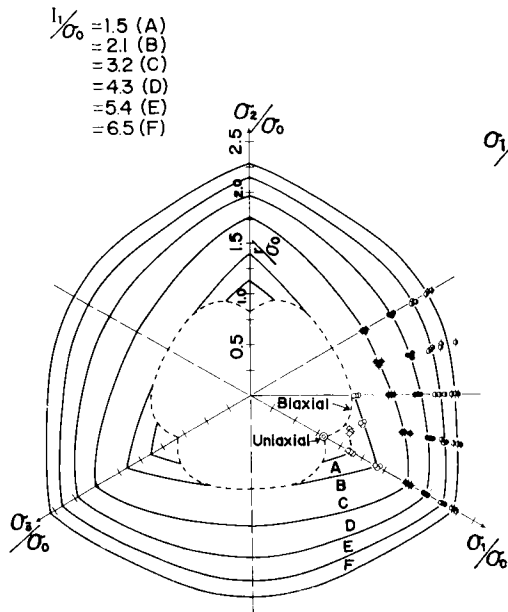


Fig. 10. Right sections.

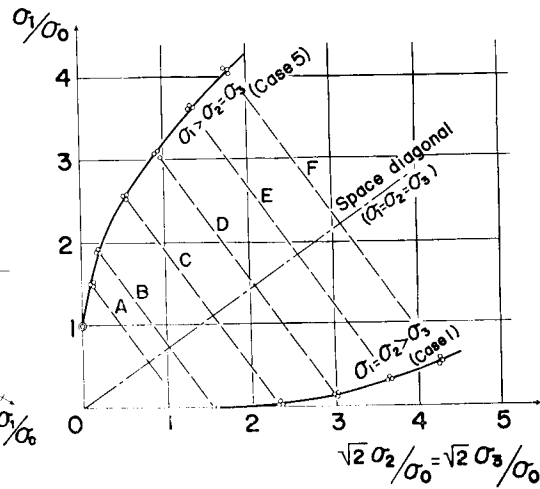


Fig. 11. Rendulic stress curves.

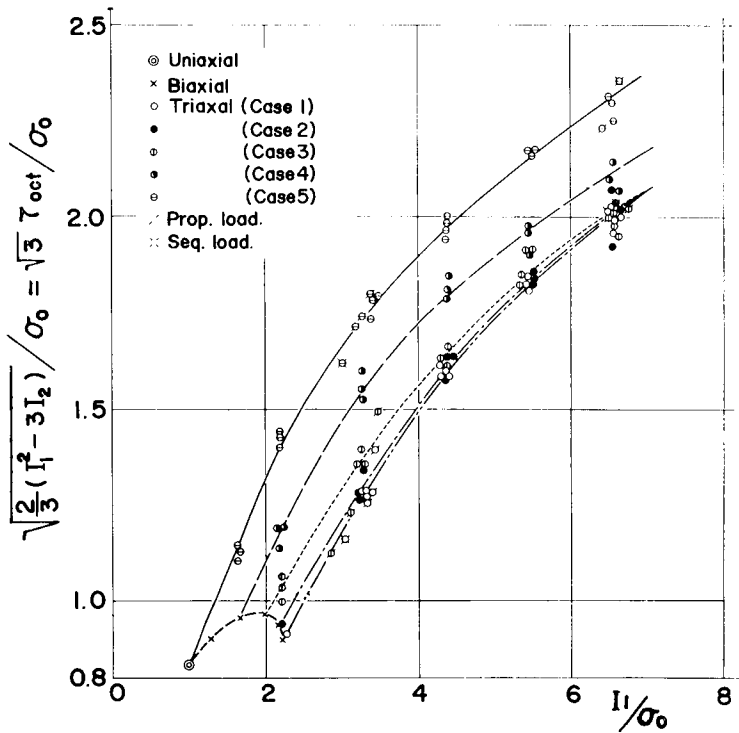


Fig. 12. Representation by octahedral stresses.

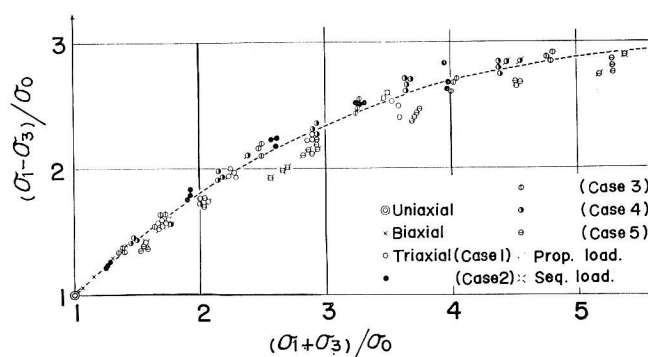
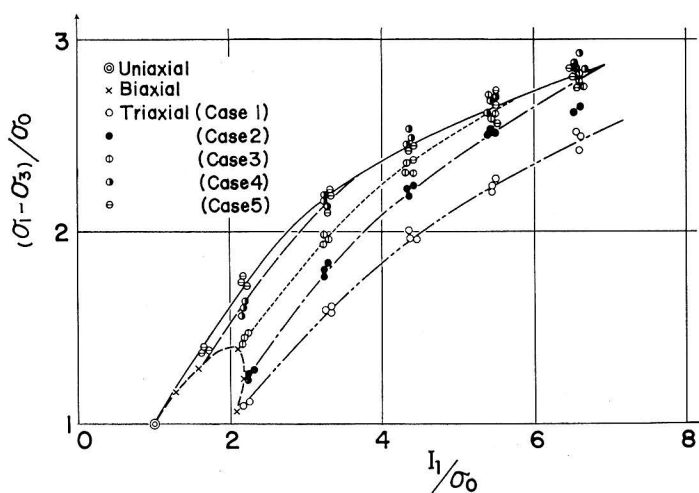
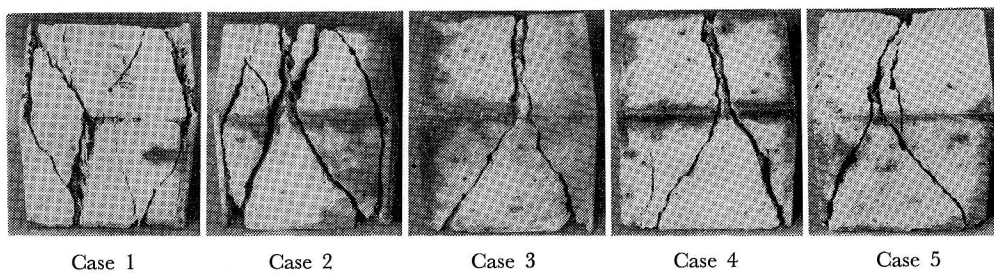
Fig. 13. Relations between  $(\sigma_1 + \sigma_3)/\sigma_0$  and  $(\sigma_1 - \sigma_3)/\sigma_0$ .Fig. 14. Relations between  $I_1/\sigma_0$  and  $(\sigma_1 - \sigma_3)/\sigma_0$ .

Fig. 15. Failure patterns (Triaxial-Series C).

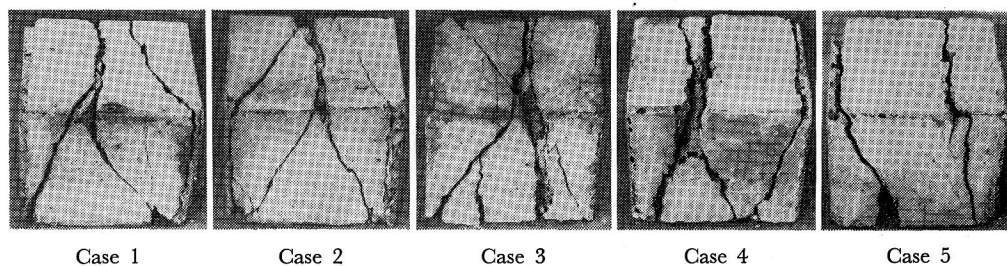


Fig. 16. Failure patterns (Triaxial-Series F).

The shape of the right sections is slightly bulged from an equilateral triangle as already discussed in 2. The sections expand and become more bulged with an increase of the sum of the principal stresses ( $I_1/\sigma_0$ ). The reason may be that the effect of flow will come into play as hydrostatic pressure increases. The effect, however, is very small in the present experimental range.

The broken lines in Fig. 10 shows the projection of the biaxial curve (Fig. 8) on the plane of  $I_1=0$  ( $\Pi$ -plane). The inside of the broken curve cannot be determined by the present test. Figs. 10 and 11 show that the expanding ratios of the right sections become smaller as hydrostatic pressure increases.

From Figs. 10 and 11 the failure surface is easily visualized as shown in Figs. 1 and 6. The surface thus obtained is the failure criterion of lightweight aggregate concrete under multiaxial compression.

Fig. 12 is the so called octahedral stress representation, in which  $\sqrt{3} \tau_{oct}/\sigma_0$  is taken as an ordinate. For the same ( $I_1/\sigma_0$ ), the ordinate is the same as ( $r/\sigma_0$ ) in Fig. 10, i.e. the ordinate corresponds to the distance between the failure surface and the space diagonal on a right section. The ordinates for the same  $I_1/\sigma_0$  are different for each case. As hydrostatic pressure increases, the ratio of  $r/\sigma_0$  between the cases approaches unity. The ratio between Case 1, 2 and 3, for example, becomes unity at  $I_1/\sigma_0 = 6.5$ . This shows that the corresponding part of the right section is a circular arc.

Octahedral shear stress criterion implies one-to-one correspondence between the values of  $\tau_{oct}/\sigma_0$  and  $I_1/\sigma_0$ , i.e. it represents a single curve. This is not valid for Fig. 11. Thus, the octahedral shear stress criterion cannot be applicable for the failure criterion of lightweight aggregate concrete.

In Fig. 13 a simple curve approximates the test results fairly well. The relation between the sum and the difference of the maximum and the minimum stresses (this does not mean that the failure occurs by maximum shear stress) is easily transformed into a failure surface in the principal stress space. Thus, the

curve in Fig. 13 can be regarded as an approximate failure criterion.

Fig. 14 does not indicate the simple relation between the maximum difference and the sum of the principal stresses. Thus, such a failure criterion is not appropriate for lightweight aggregate concrete.

Judging from Figs. 12 and 13 the loading path has no significant effect on the failure criterion in the present experimental range.

As shown in Figs. 15 and 16, the cracks of Cases 1 and 2 appeared in several oblique planes to all the principal directions, whereas those of Cases 3, 4 and 5 in two planes containing the intermediate stress. The inclinations of the formers are between  $20^\circ$  and  $27^\circ$  from the normal plane of the minimum principal stress, whereas those of the latters are between  $20^\circ$  and  $30^\circ$  from the direction of the maximum stress. These angles, however, do not correspond to the slip angles of Mohr's criterion. Judging from this fact and that lots of aggregates were split in the cracked planes, the planes may be interpreted as fractured by tensile strain and then slipped. Thus, the angles obtained cannot be regarded as internal angles of friction.

## 5. Conclusions

The following can be concluded.

(i) A failure criterion of macroscopically isotropic and homogeneous brittle materials is expressed in the principal stress space by a convex surface with space diagonal of its three-fold rotation axis. The surface expands with decreasing ratio as hydrostatic pressure increases.

The right sections of the surface are slightly bulged from equilateral triangles and become more bulged with an increase of hydrostatic pressure.

Rendulic stress curves may be approximated by parts of parabolas.

(ii) Biaxial failure criterion is the intersection of the failure surface and a plane of zero minimum stress.

(iii) The failure condition can be approximated by a simple curve expressed as a function of the sum and the difference of the maximum and the minimum stresses.

(iv) Loading path has no significant effect on the failure criterion of lightweight aggregate concrete in the present experimental range.

(v) The existence of the angle of internal friction cannot be confirmed.

(vi) The friction between the platen and the end surface of specimens plays an important role in compression tests, especially of cube specimens. Special care should be exercised to diminish the friction.

### **Acknowledgement**

The authors express their gratitude to Mr. Ken-ichi Hirashima, a graduate student, for his assistance in experiment.

### **References**

- 1) Niwa, Y. and S. Kobayashi: Memo. Faculty of Eng., Kyoto Univ., **29**, 1 (1967)
- 2) Niwa, Y. and S. Kobayashi: J. Soc. Materials Science, Japan, **16**, 1 (1967), (in Japanese)
- 3) Niwa, Y., W. Koyanagi and S. Kobayashi: Trans. Japan Soc. Civil Eng., (in Japanese), (in press)